JOURNAL OF GUIDANCE, CONTROL, AND DYNAMICS
Vol. 20, No. 4, July–August 1997

Separation Dynamics of Strap-On Boosters in the Atmosphere

Rajeev Lochan* and V. Adimurthy†
Vikram Sarabhai Space Center, Trivandrum 695022, India
and
K. Kumar‡
Indian Institute of Technology, Kanpur 208016, India

The dynamics associated with the jettisoning of a strap-on booster from the parent launch vehicle is investigated. The present analysis accounts for experimental aerodynamics of separation utilizing a two-step method that employs a wind tunnel in a problem-solving mode. The first step consists of collecting wind-tunnel test results at a large number of points in the multidimensional space of independent variables. A suitable approach for surface fitting to the data leads to empirical models of the aerodynamic behavior, which are used in numerical simulations to design the appropriate separation system. The suitability of this design is examined, as a second step, through extensive simulations using the wind tunnel as a hardware subroutine to generate aerodynamic forces and moments. Two strap-on booster configurations are used for illustration.

Nomenclature

C_i^j = ith aerodynamic coefficient for the jth body, with i from 1 to 6
D_{ref}, S_{ref} = reference values for distance and surface area, respectively, for nondimensionalization
F_i^j, M_i^j = resultant force and moment components, respectively, on the body j along the X_i axes
I^j = principal mass moments of inertia of the jth body
i, j = indices representing the coordinate axes and the bodies, respectively
k = index
ℓ = $\max(\ell_1, \ell_2)$
ℓ_0 = distance of the base of the core from its own mass center; Fig. 1
ℓ_1, ℓ_2 = distances of nose of the booster and its base from its own mass center
M_∞ = freestream Mach number
m^j = mass of the jth body
n = number of bodies including the core
Q_w = dynamic pressure
r^j, χ^j, h^j = cylindrical coordinates of the instantaneous mass center of the body j with respect to C frame
T_{off} = tailoff thrust
t = time since initiation of separation
v^j = velocity of the jth body with respect to the C frame expressed in B^j frame
X_{C1}, X_{C2}, X_{C3} = local core inertial frame, C frame
X_{S1}^j, X_{S2}^j, X_{S3}^j = local strap-on inertial frame, S^j frame
X_1^j, X_2^j, X_3^j = body fixed frame associated with the jth body, B^j frame
x_i^j = instantaneous position of the mass center of the jth body referred to S^j frame
x_r, y_r, z_r = rig setting parameters; Fig. 3
α_s^j, β_s^j = two angles representing the orientation of the longitudinal axis of the jth strap-on with respect to the C frame; Fig. 1
α_w, β_w = pitch and yaw angle of attack, respectively; Fig. 1
δ_1, δ_2, δ_3 = rig setting constants; Fig. 3
ϵ = Levi-Civita density function
θ_1^j, θ_2^j, θ_3^j = Eulerian angles representing the attitude of the body j
θ_r, ψ_r = rig setting angles; Fig. 3
θ_w, Φ_w = angle of incidence and wind plane angle, respectively; Fig. 1
ρ = spring precompression
σ = model scale for scaled down model, > 1
ω = angular velocity

Subscripts

a = aerodynamics
$(\ )_{\max}$ = maximum value of $(\ )$
$(\ )_{\text{ref}}$ = reference value of $(\ )$ for nondimensionalization
$(\ )_0$ = value of $(\ )$ at the initiation of separation
s = separation system
t = thrust and/or residual thrust
$\Delta(\ )$ = change in $(\ )$

Received March 15, 1995; revision received March 11, 1997; accepted for publication April 7, 1997.

*Chief, Separation Dynamics Section, Flight Mechanics Division.
†Group Director, Aero and Flight Dynamics Group.
‡Professor, Department of Aerospace Engineering. Associate Fellow AIAA.

Introduction

THE general dynamics of separating bodies has received the attention of several investigators.[1–6] The problem of strap-on booster separation, however, has received little attention. Although a number of countries have been using strap-on technology for years, no directly related investigations appear to have been reported in the open literature until recently. Even though Prahlad[7] and Sundaramurthy et al.[8] have touched on some of its aspects, the first systematic attempt to analyze this problem was made by the present authors.[9] Analyzing the geometry of collision in a multibody system, the authors have developed three different approaches for detection of collision[9] and have constructed a no-collision domain in design parameter space. A novel approach is adopted to decouple separation dynamics from the core control dynamics, leading to considerable simplification. The present paper represents a systematic attempt to incorporate the important aspect of separation aerodynamics in the design analysis that has previously been ignored.

The aerodynamics of separation is rather complex due to relatively large angles of incidence, intricate geometry, and the involved interference phenomenon. Recently, there have been some attempts to simulate this complex flowfield. Moraes et al.[10] developed the Navier–Stokes code that provided a good agreement with the experiments but only on the nose part of the on-going stage. A more successful attempt seems to have been made by Singh et al.,[11] who employed a second-order explicit predictor–corrector method using MacCormack's shock-capturing scheme together with overlapping

grids to solve Euler's equations for zero angle of incidence. Evidently, these results cannot be applied in the present situation because the angles of incidence can be significantly high, further accompanied by changing orientations of the separating bodies. This as well as similar subsequent attempts at purely theoretical treatment of separation aerodynamics,[12] therefore, appear to be totally inadequate.

A considerable amount of aerodynamic data[13,14] including stability derivatives[15] has been generated for Space Shuttle-type configurations involving winged bodies. The data have been utilized for separation dynamics investigations.[16,17] Lanfranco[18] has investigated dynamics as well as aerodynamics of separation using a captive trajectory system. These earlier investigations are related to the separation of two similar-sized bodies of fully reusable, partially reusable (like the current Space Shuttle), and ferry types of configurations. These have been effectively summarized by Decker and Wilhite.[19] In contrast, not much is available in the open literature on aerodynamics of strap-ons separating from the conventional launch vehicles. The aerodynamic characteristics here are far different from those of the reusable vehicles. This problem is also different from separating an external store from the parent aircraft. Although the experimental results provided by Moraes et al.[10] come closer to the geometry at hand, the emphasis lies mainly on the aerodynamic characteristics of the core in the presence of boosters. This, however, is of little interest to the present problem. From a separation viewpoint, more pertinent test results comprising axial force, side force, and yaw moment coefficients for two equal-sized boosters have been presented by Sundaramurthy et al.[8]

Formulation

The details of formulation of the equations of motion are given in Ref. 9. Therefore, it is sufficient to state the governing equations of motion as follows:

$$\dot{v}_i^j - \epsilon_{ik\ell} v_k^j \omega_\ell^j = F_i^j \Big/ m^j \qquad i = 1, 2, 3 \tag{1}$$

$$I_i^j \dot{\omega}_i^j - \epsilon_{ik\ell} I_k^j \omega_k^j \omega_\ell^j = M_i^j \qquad i = 1, 2, 3 \tag{2}$$

where the external force F_i^j and moment M_i^j are given by

$$\left.\begin{aligned} F_i^j &= F_{ti}^j + F_{si}^j + F_{ai}^j \\ M_i^j &= M_{ti}^j + M_{si}^j + M_{ai}^j \end{aligned}\right\} \qquad \begin{aligned} &i = 1, 2, 3 \\ &j = 1, 2, 3, \ldots, n \end{aligned} \tag{3}$$

and models for forces and moments due to thrust, the residual thrust, and spring force were developed in Ref. 9.

Aerodynamics of Separation

The aerodynamic forces and moments on the body j along the ith axis of its own body frame are expressed as follows:

$$\left.\begin{aligned} F_{ai}^j &= Q_w S_{\text{ref}} C_i^j \\ M_{ai}^j &= Q_w S_{\text{ref}} D_{\text{ref}} C_{i+3}^j \end{aligned}\right\} \qquad \begin{aligned} &j = 1, 2, 3, \ldots, n \\ &i = 1, 2, 3 \end{aligned} \tag{4}$$

where D_{ref} and S_{ref}, used as convenient references for distance and surface area, respectively, correspond to the strap-on diameter and its cross-sectional area. The aerodynamic coefficients C_i^j denote the force coefficients for the values 1, 2, and 3 for i, whereas the values 4, 5, and 6 represent the moment coefficients corresponding to the X_1, X_2, and X_3 axes, respectively (see Appendix). The entire problem of separation aerodynamics thus reduces to providing models or algorithms for computation of these coefficients.

Several simplifying assumptions are made to render the problem tractable. Freestream Mach number, dynamic pressure, and external flow are assumed to remain unaltered during the separation process. Hence, the change in the angle of incidence results only from the change in the orientation of the separating body. A rather short duration of the separation process spanning less than half a second justifies these assumptions. Furthermore, the minor asymmetries in the geometry of the strap-on due to attachments/protrusions are ignored.

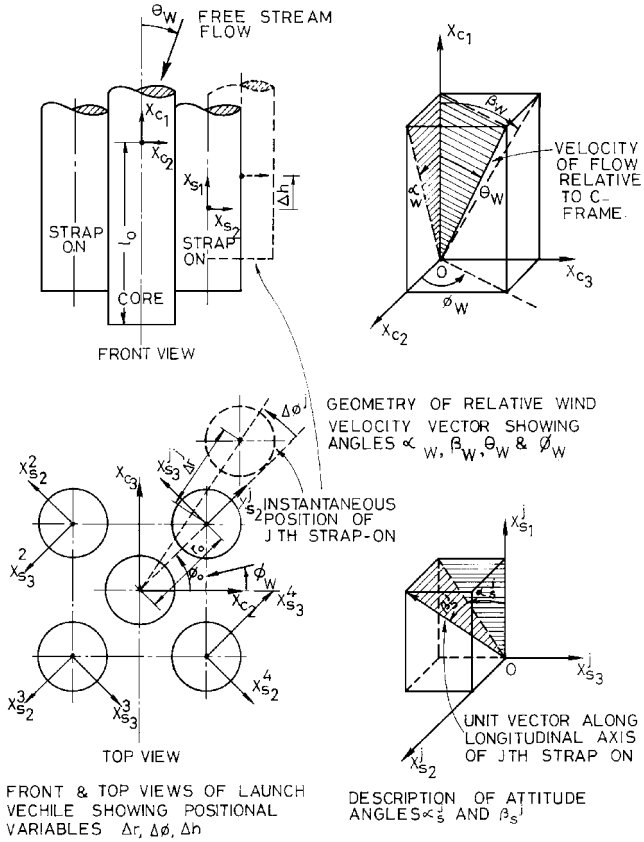

Fig. 1 Description of various coordinate frames and aerodynamic state variables.

Figure 1 describes the various aerodynamic variables required to express the aerodynamic forces and moments. The external flowfield is specified in terms of two angles, θ_w and Φ_w. Of these, θ_w, called the angle of incidence, represents the included angle between the X_{C1} axis and the relative wind velocity vector, whereas the wind plane angle Φ_w denotes the angle made by the velocity component in the $X_{C2}X_{C3}$ plane with the X_2 axis. The pitch angle of attack α_w and the yaw angle of attack β_w are related to these two angles as

$$\alpha_w = \arctan(\tan\theta_w \cos\Phi_w) \qquad \beta_w = \arctan(\tan\theta_w \sin\Phi_w) \tag{5}$$

Inversely,

$$\theta_w = \arctan\left[\left(\tan^2\alpha_w + \tan^2\beta_w\right)^{\frac{1}{2}}\right] \qquad \Phi_w = \arctan\left(\frac{\tan\beta_w}{\tan\alpha_w}\right) \tag{6}$$

Although it is possible to estimate the bounds on θ_w in flight, the estimation of the wind plane angle may not be easy as the latter is governed by the attitude errors and local wind conditions prevailing at that altitude. In addition to these two parameters of the overall system, two parameters describing the orientation of the longitudinal axis of a booster prove useful in subsequent analysis. Let these be denoted as α_s^j and β_s^j. These are now expressed in terms of the corresponding attitude parameters

$$\alpha_s^j = \arctan\left(\frac{\tan\theta_2^j}{\cos\theta_3^j}\right) \qquad \beta_s^j = \arcsin\left(\cos\theta_2^j \sin\theta_3^j\right) \tag{7}$$

Here, attention is focused on developing a sufficiently accurate description of the aerodynamic forces and moments in a suitable form facilitating design of the separation system. For this specific objective at hand, a more general and precise treatment for a complete comprehension of the complex aerodynamic issues is not essential.

For discussion of the methodology, we consider a core with two boosters with all of the bodies having the same diameter in a supersonic flow. Each of the strap-ons is assumed to be attached to the

core through a set of four springs, two near the top end and two near bottom. The design problem can now be stated as follows.

Design Problem

The design objective is to determine the spring characteristics such that for

$$M_{\min} \le M_\infty \le M_{\max} \qquad -\alpha_{\max} \le \alpha_w \le \alpha_{\max}$$
$$-\beta_{\max} \le \beta_w \le \beta_{\max} \qquad T_{\text{off}} \le T_{\max} \qquad Q_w \le Q_{\max} \tag{8}$$

the separation of the strap-ons from the core is ensured without any mechanical interference. This paper aims at evolving a strategy for design of the springs so as to meet this requirement.

Evidently, the aerodynamic coefficients for, e.g., the jth strap-on, would be influenced by the aerodynamic state variables of other strap-ons as well. Hence, in general, symbolically

$$C_i^j = C_i^j\left(M_\infty, \theta_w, \Phi_w, \Delta r^j, \Delta \chi^j, \Delta h^j, \alpha_s^j, \beta_s^j, \Delta r^k, \Delta \chi^k, \Delta h^k, \alpha_s^k, \beta_s^k\right) \tag{9}$$

with k representing all of the other strap-ons. Naturally, such a relationship depends on the geometries of the separating bodies.

To deal with the various issues involved, a two-step procedure is proposed. The first one, hereafter called grid approach, consists of aerodynamic data generation through wind-tunnel tests by making measurements at judiciously chosen discrete aerodynamic states and evolving a reasonably accurate empirical model representing the aerodynamic behavior of the separating strap-ons. This model, then, is utilized to arrive at a suitable design for the springs, through extensive numerical simulations. This is followed by the second step, hereafter referred to as the time march approach, which attempts at verification of the design through more accurate simulations using the wind tunnel as a hardware subroutine. This technique is known as the semicaptive trajectory technique.[20]

Grid Approach

The grid approach involves building an empirical aerodynamic model from the experimentally determined data at well-designed grid points of independent aerodynamic states. We aim at developing the two extreme trajectories within which the actual path of the separating strap-ons will lie.

To limit the wind-tunnel run time to a minimum, several simplifying assumptions are made. All strap-on separation events are in supersonic regimes, far away from the transonic Mach numbers. Furthermore, the Mach number variation itself is usually small and, hence, has little effect on the aerodynamics.

It may be seen that, for the system under consideration, a strap-on may collide with the core in two possible ways, with either the nose or the base of the strap-on hitting the core. Therefore, one aims at synthesizing the extremes of these two cases. In keeping with the earlier approach of a simplified treatment in the first phase, we assume the wind velocity vector to be lying in the plane $X_{C1}X_{C2}$ as the basis for a conservative design. Therefore, it is apparent that aerodynamic out-of-plane forces and moments would be negligible. Also, the misalignments of the strap-on tailoff thrust vector and that of the separation mechanism would be confined to the yaw plane for the synthesis of the most adverse situation. As a result, the dynamics under consideration becomes planar. Further, in general, the aerodynamics is expected to change monotonically with the angle of incidence, as is later confirmed through experiments, and therefore, it would suffice to consider only the two extreme angles of incidence. Thus, if we can ensure collision-free separation for the case $\Phi_w = 0$ and $\theta_w = \theta_{\max}$ that is likely to lead to avoidance of collision in virtually all cases involved, then

$$0 \le \Phi_w \le \pi \qquad \text{and} \qquad -\theta_{\max} \le \theta_w \le \theta_{\max} \tag{10}$$

For cases $\Phi_w \neq 0$ deg, the out-of-plane aerodynamic force and moment components induce a general three-dimensional motion; nonetheless, it is not expected to make the collision between the separating bodies any more likely. From a few experimental results shown in Fig. 2, it is evident that the side force coefficient C_2 for the windward booster remains virtually unaffected by the change in

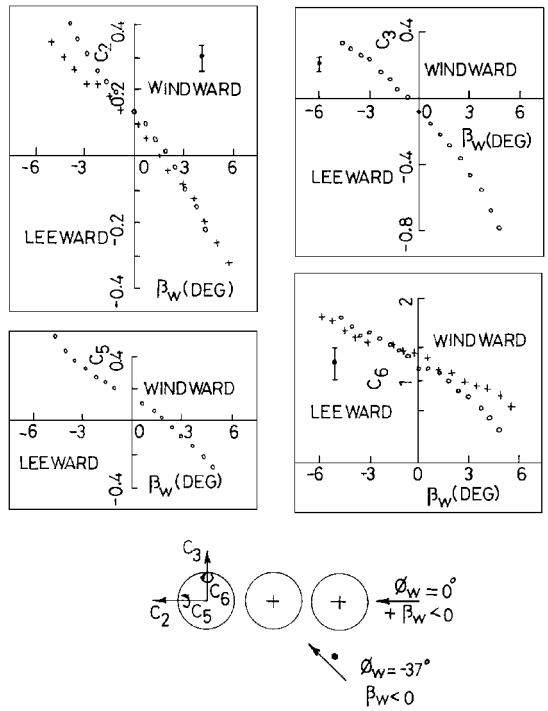

Fig. 2 Influence of the wind plane angle over the aerodynamic coefficients of the separating strap-ons.

wind plane angle, whereas that for the leeward strap-on shows some improvement when Φ_w is different from 0 deg although not exceeding the error bar. The yaw moment coefficient C_6, however, displays an opposite trend, again within the measurement uncertainty. Naturally, worst dynamics of the windward booster will result from $\Phi_w = -37$ deg, whereas the same for the leeward will require $\Phi_w = 0$ deg. Nevertheless, we proceed with the assumption that the yaw plane aerodynamics will not be affected by the pitch angle of incidence for the preliminary design purposes. Naturally, only three aerodynamic coefficients, C_1, C_2, and C_6, and three aerodynamic state variables, Δr, β_s, and Δh, are now of significance.

To minimize the wind-tunnel test program, the physical range of interest for the various parameters is chosen. A consideration of the geometry of the separating bodies leads to the following range for Δr and Δh:

$$\Delta r \le \ell \qquad \text{and} \qquad -\Delta h \le \ell + \ell_0 \tag{11}$$

The estimation of the range of β_s is much more involved due to a large number of factors, e.g., dynamic pressure, geometry, etc., that influence its growth in the time interval of interest dictated by the mentioned geometrical inequalities. A trial-and-error approach is required to ascertain limits on β_s.

These ranges and the geometric configurations are adequate for the design of a rig setting mechanism to realize these parameters in a wind tunnel. A simple and cost-effective design was developed by Sundaramurthy et al.[21] A schematic is reproduced here in Fig. 3 defining the rig setting parameters. The relationship between the rig setting parameters x_r, y_r, z_r, θ_r, and ψ_r and the corresponding aerodynamic state variables for the configuration under consideration can be easily obtained geometrically:

$$\theta_r = -\alpha_s \qquad \psi_r = \beta_s \qquad y_r = -\Delta h/\sigma - \delta_3 \sin\psi_r$$
$$z_r = [(r_0 \cos\chi_0 - r\cos\chi)/\sigma - \delta_1 \sin\theta_r - \delta_2(1-\cos\theta_r) - \delta_3 \cos\psi_r \sin\theta_r]/\cos\theta_r \tag{12}$$
$$x_r = -\Delta h/\sigma - \delta_1(1-\cos\theta_r) + (\delta_2 - z_r)\sin\theta_r + \delta_3(1-\cos\psi_r\cos\theta_r)$$

A typical set of parametric combinations in the Δr–β_s plane chosen for the wind-tunnel test runs on the basis of several practical physical

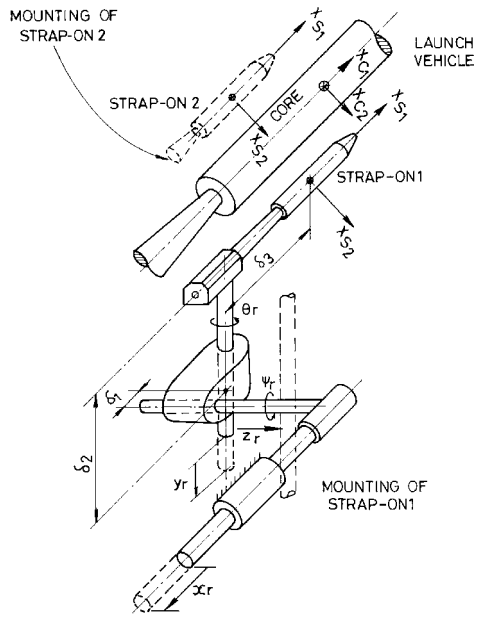

Fig. 3 Rig setting mechanism.

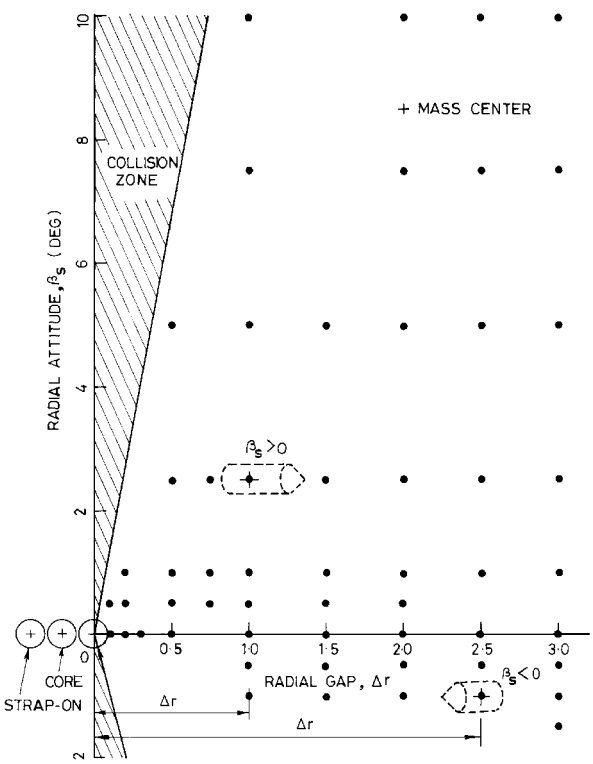

Fig. 4 Typical grid pattern in Δr–β_s.

constraints is shown in Fig. 4. These appear in the form of a grid. A judicious choice of such a grid pattern is crucial to the development of an effective empirical model. The various points in the grid are so chosen as to capture the essential characteristics, such as far-field and near-field behavior, adequately.

This entire grid pattern corresponds to one particular value of Δh, e.g., 0. To include the effects of the variation of the longitudinal gap, the data for the same pattern may have to be obtained at different values of Δh. This not only increases the number of blowdowns considerably but also complicates the surface fitting exercise. As a first step, it is now proposed to measure the influence of Δh at only one Δr–β_s combination, e.g., initial, and use the same effect all over for preliminary design. Although not strictly valid, we accept these simplifying assumptions merely as a first step.

As yet another simplification, although not truly valid (Fig. 5), we assume that the aerodynamic behavior of every strap-on remains

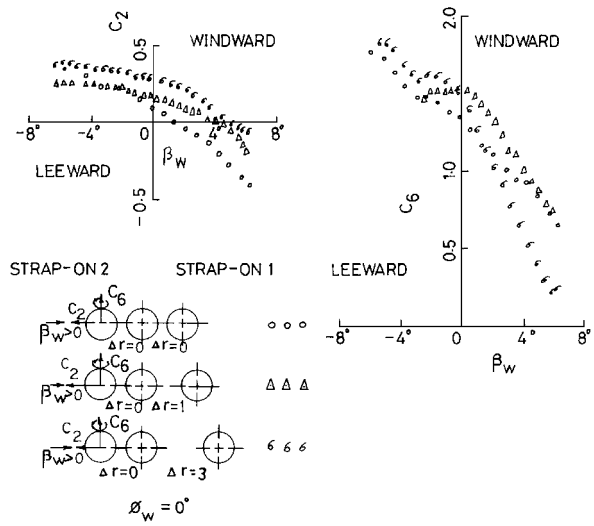

Fig. 5 Influence on the aerodynamic characteristics of a strap-on due to the variation of Δr for the other.

unaffected by the changes in the position or orientation of the others. This assumption, however, would be relaxed later in the second step when the validity of the design would be tested. The empirical model under consideration then takes the following simplified form:

$$C_i^j = C_i^j(\Delta r, \beta_s, \Delta h) \qquad i = 1, 2, \text{and } 6 \tag{13}$$

at $\Phi_w = 0$ and $\theta_w = \pm\theta_{\max}$.

In view of this assumption, it is now possible to maximize the data in each blowdown by instrumenting the two strap-ons and placing them so as to cover two different grid points. Considerations of symmetry then enable transfer of data collected for one strap-on to that of the other as

$$C_i^2(\Delta r, \Delta\chi, \beta_s)|_{\theta_w} = C_i^3(\Delta r, \Delta\chi, \beta_s)|_{-\theta_w}$$
$$i = 1\text{–}6 \qquad \text{and} \qquad \Phi_w = 0 \tag{14}$$

Surface fitting to the ensemble of the aerodynamic coefficients over the numerous grid points as already discussed, we obtain the following empirical relations for $\Phi_w = 0$ deg required for numerical simulations.

Strap-on 1 (body 2):

$$C_1^2 = -1.1 - 0.02\Delta r - 0.01\beta_s$$
$$C_2^2 = 0.23 + 0.25\Delta r - 0.04\Delta r^2 - 0.002\Delta r^3 + 0.125\beta_s + 0.005\beta_s^2 \tag{15}$$
$$C_6^2 = 1.05 + 2.23\Delta r - 1.6\Delta r^2 + 0.3\Delta r^3 + 0.1\beta_s + 0.005\beta_s^2 - 0.08\Delta h$$

Strap-on 2 (body 3):

$$C_1^3 = -1.12 + 0.01\Delta r - 0.005\beta_s$$
$$C_2^3 = -0.26 - 0.02\Delta r - 0.004\Delta r^2 - 0.0007\Delta r^3 + 0.125\beta_s - 0.001\beta_s^2 \tag{16}$$
$$C_6^3 = 0.08 - 1.1\Delta r + 0.5\Delta r^2 - 0.07\Delta r^3 + 0.2\beta_s - 0.05\Delta h$$

where β_s is in degrees and all of the distances are normalized with respect to D_{ref}.

The numerical simulations enable us to arrive at a physically realizable set of springs, which ensure a collision-free separation with a wide margin of safety. Needless to say, the design must ensure that the nose, as well as the base of either of the strap-ons, does not hit the core even if the uncertainties in aerodynamic measurements and the resulting aerodynamic model combine with the environmental parameters in the worst possible way.

For a system with parameters as shown in Table 1, the application of the grid approach results in a realizable separation system described in the same table. The scenario of the falling strap-ons is as shown in Fig. 6. To show the effect of aerodynamics, the case with no aerodynamics is included.

Time March Approach

The set of physically realizable spring parameters obtained through the grid approach must now be validated, especially in view of the various simplifying assumptions made in the first step. The initial data together with the system parameters thus obtained serve here as the inputs required to initiate an accurate simulation for this purpose. The simplifying assumptions are no longer needed. The wind-tunnel run for the model configuration corresponding to this known initial state generates the aerodynamic data to be utilized off-line for the computer run at this initial time step, which in turn enables computation of the rig setting parameters corresponding to the new configuration of the separating bodies for the subsequent blowdown. Thus, the stage is set for repeating this process for the next step, which begins with the wind-tunnel run after manually changing the model setting to the one just predicted. This process of marching in time from an earlier step to the next is continued until we are able to ascertain separation with or without collision (Fig. 7).

The interval for each time march step must be carefully chosen. It decides the instants at which the aerodynamic data are sampled through wind-tunnel test runs. For the gradually changing system configuration, even larger step size may suffice. In case of rapidly varying configurations, however, the aerodynamic data must be sampled more frequently and, hence, relatively smaller step sizes must be used. Thus, the step size may depend on the initial system parameters as well as the time elapsed during the separation process. Moreover, smaller step size, although capable of capturing aerodynamic behavior more faithfully, would be more susceptible to errors in model setting and the resulting measurement noise. A suitable compromise needs to be struck between these conflicting requirements. For the systems considered here, initially, a step size of 40 ms was found suitable. For reasons explained earlier, this had to be

Table 1 Parameter values for the illustrative example

Configuration: Core with two boosters, all of equal diameters		
Mass of core		17,000 kg
Thrust on core (constant, corrected for atmospheric pressure)		365 kN
Each strap-on booster		
Mass		2,900 kg
Mass moment of inertia		700, 33,000, 33,000 kgm^2
Leftover thrust		3 kN
Nozzle cant		10 deg
Thrust location		4 m below the mass center
$\ell_0 = 9.35$ m	$\ell_1 = 6.25$ m	$\ell_2 = 4.25$ m
$r_0 = 1.15$ m	$h_0 = -4.75$ m	
Aerodynamics		
$Q = 55$ kPa	$S_{\text{ref}} = \pi/4$ m^2	$D_{\text{ref}} = 1$ m
$M_\infty = 2.4$	$C_1^1 = -0.75$	
Range of angle of incidence, deg $-3 \le \alpha_w \le 3$ and $-4 \le \beta_w \le 4$		
Separation system (derived using grid approach and subsequently confirmed through time march approach)		
Number of identical springs for each strap-on = four; two near the top and two near the base		
Load deflection relation for each spring (P, kN and δ, m)		
$P(\delta) = 3.5 + 750\delta - 80\delta^2$		
$0 \le \delta \le \rho$ and $\rho = 0.11$ m		

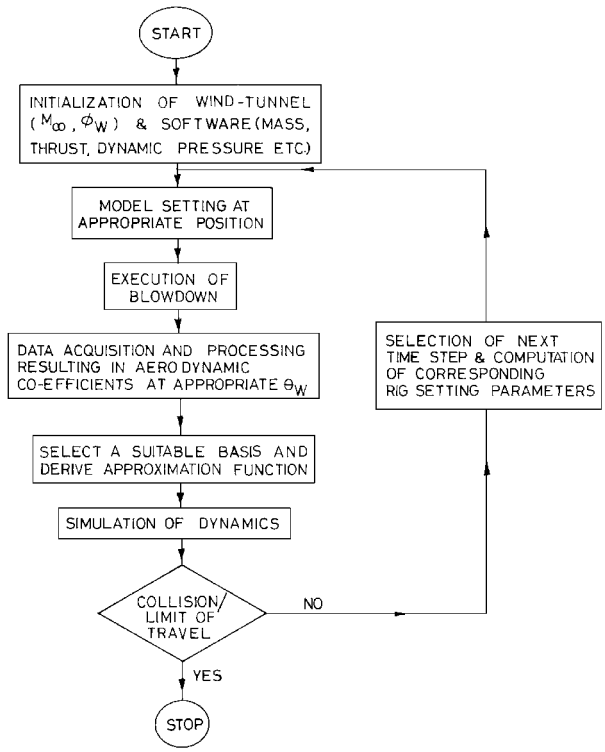

Fig. 7 Flow chart showing sequence of steps in time march approach.

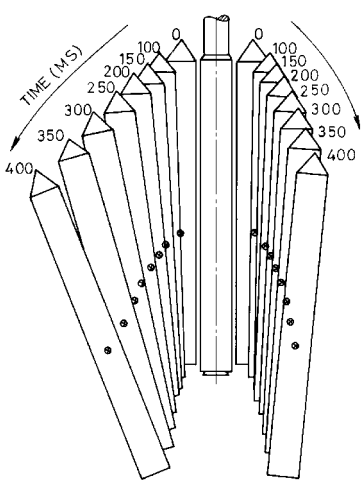

a) With aerodynamics (Q = 55 kPa)

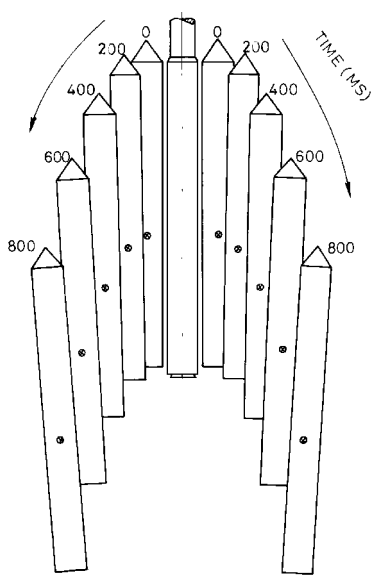

b) Without aerodynamics (Q = 0)

Fig. 6 Trajectories for the separating strap-ons.

gradually reduced to 20 ms at the end of the simulation. The stability, convergence, and accuracy of the numerical integration of the governing equations require the integration step to be much smaller (≈1 ms) compared to the step size at which blowdowns are conducted. Therefore, some suitable interpolation/extrapolation schemes would also be needed to compute required aerodynamic coefficients at desired close integration steps from blowdowns conducted at coarse time march steps. A judicious choice of reference variable for this purpose enables a more effective utilization of the sampled data. The comparison between the extrapolation and the subsequent blowdown provides an in-built mechanism to regulate the time march step size.

The numerical simulation duly accounts for the core thrust and the tailoff thrust of the strap-ons in addition to the aerodynamic effects discussed earlier. The pertinent details of the models for separation systems, residual thrusts, and the methods of detection of collisions, if any, used in the analysis are available elsewhere.[9]

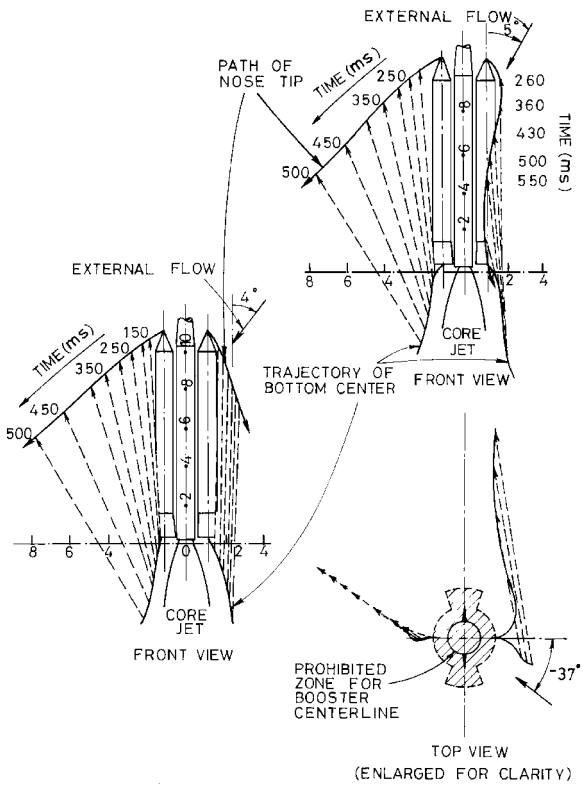

a) $\Phi_w = 0$ deg **b) $\Phi_w = -37$ deg**

Fig. 8 Simulation results for a two-booster configuration confirming collision-free separation.

Results and Discussion

For the results presented here, the wind-tunnel tests were conducted at the 1.2-m trisonic facility of National Aerospace Laboratories, Bangalore, India. For the system under consideration, the system parameters are defined in Table 1, wherein the separation system obtained from the grid approach is also included. The simulation results obtained with a view to validating the configuration developed in the first step are generated through a time march approach. The results are provided for two wind plane angles (Fig. 8). If desired, more cases can be examined to achieve full confidence in the design.

The simulations undertaken here clearly suggest ever present large clearances that ensure a collision-free separation with a wide margin of safety. The angle $\Phi_w = 0$ deg corresponds to the case of relative motion in a single plane. However, the case $\Phi_w = -37$ deg (Fig. 8b) leading to a general three-dimensional motion demands the clearances in both the views as shown here. It may not always be possible to ensure a nose opening rotation for the boosters under all possible circumstances due to various geometrical and physical constraints on the implementable separation system. Although a nose closing rotation of the windward booster is evident here, a minimum physical clearance, under the worst possible combination of environmental parameters and the aerodynamic modeling uncertainty, beyond $0.25 D_{\text{ref}}$ was considered adequate. The presence of additional attachments on the core, e.g., fins, enlarges the prohibited region that must not be violated by the strap-on axis of symmetry. This enlargement can be obtained through simple geometric consideration of the sizes and the core attitude excursion, if any.

On the other hand, should any simulation run lead to the occurrence of collision between any two separating bodies, the preliminary design of the separation system should be suitably altered and subsequently confirmed using the described approach.

In the second example, we consider a more complex situation of a launch vehicle with six strap-ons, of which only four are jettisoned. Unlike in the preceding configuration, here we must also ensure that the separating strap-ons do not hit the nonseparating adjacent ones. The number of modes of possible collision has now gone up to four. Accordingly, while using the grid approach of the first step, additional wind plane angles need to be considered to cover the new possibilities. Figure 9 shows the results of the simulation using the time march approach for one wind plane angle only. Collision-free separation is evident for this case. Simulation runs for other critical cases, not shown here, also confirm the suitability of the design chosen.

The suitability of the preliminary design obtained in the first step has been invariably confirmed. The methodology proposed here has already been proven in successful flights of the Indian launchers

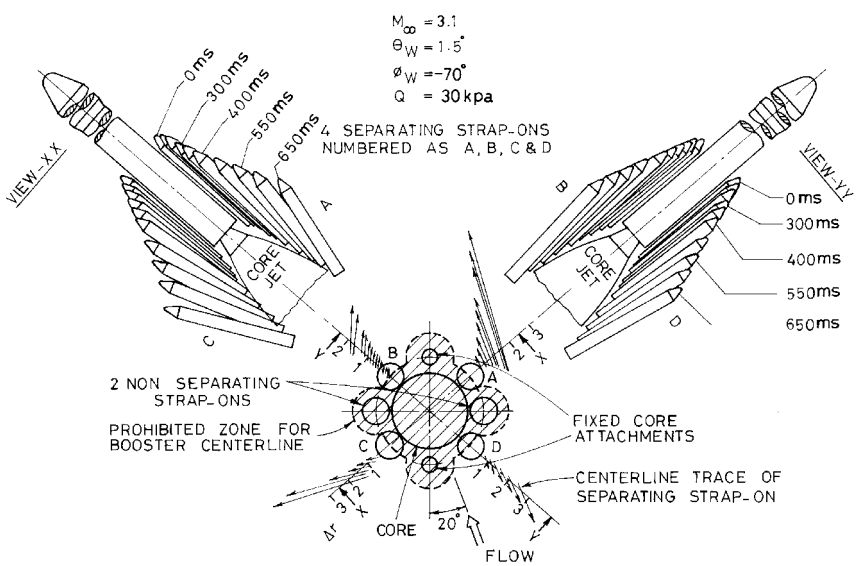

Fig. 9 Simulation results for a six-booster configuration confirming collision-free separation.

ASLV (Augmented Satellite Launch Vehicle) and PSLV (Polar Satellite Launch Vehicle).

Appendix: Frames of Reference

The coordinate systems used for convenience of representation and interpretation are described.

1) Local core inertial frame $X_{C1}X_{C2}X_{C3}$ (C frame) with origin frozen at the center of mass at $t = 0$ and taking the axis X_{C1} along the longitudinal axis, X_{C2} along the pitch axis, and X_{C3} was chosen so as to complete the right-handed triad (Fig. 1). This frame is assumed to move with uniform system velocity taken at $t = 0$. Because, at this instant, the core and the strap-ons have the same orientation and velocity with reference to this C frame, the initial conditions of velocity and orientation for all of the bodies reduce to zero. The velocity of the core (and all other bodies), however, may evolve with time under the influence of external forces.

2) Local strap-on inertial frames $X^j_{S1}X^j_{S2}X^j_{S3}$ (S^j frame) for the jth strap-on, with origin at its own center of mass at $t = 0$, X^j_{S1} was taken parallel to X_{C1}, X^j_{S2} along the radial direction, and X^j_{S3} was selected so as to complete the right-handed triad as before (Fig. 1).

3) Body frame $X^j_1X^j_2X^j_3$ (B^j frame) for the jth body was such that the frames B^j and S^j are identical at $t = 0$.

The body frames are introduced to facilitate the Eulerian description of angular motion. These noninertial frames are obtained from the inertial S^j frames (C^1 frame) by three successive rotations in the following sequence: 1) a rotation of θ^j_3 about the X^j_{S3} axis (X_{C3} axis) leading to intermediate frame $(X'_1X'_2X'_3)$, 2) a rotation of θ^j_2 about the X'_2 axis leading to another intermediate frame $(X''_1X''_2X''_3)$, and, finally, 3) a rotation of θ^j_1 about the X''_1 axis leading to the body frame $X^j_1X^j_2X^j_3$.

The origin of the S^j frame, the mass center of the body j at $t = 0$, is referred to the C frame in terms of the radial distance r^j_0, the angular distance χ^j_0, and the longitudinal location h^j_0. The S^j frame is obtained from the C frame by a single rotation of χ^j_0 about the X_{C1} axis leading to a time-independent transformation matrix relating the two. The parameters, representing the mass center of the body j at some general time t, are referred to as r^j, χ^j, and h^j. The instantaneous change in the position of the mass center of the jth body, represented by $\Delta r^j, \Delta \chi^j$, and Δh^j, is then given by

$$\Delta r^j = \left\{\sqrt{\left(r^j_0 \cos\chi^j_0 + x^j_2\right)^2 + \left(r^j_0 \sin\chi^j_0 + x^j_3\right)^2}\right\} - r^j_0$$

$$\Delta \chi^j = \arctan\left\{\frac{r^j_0 \sin\chi^j_0 + x^j_3}{r^j_0 \cos\chi^j_0 + x^j_2}\right\} - \chi_0 \qquad \Delta h^j = x^j_1 - h^j_0$$

Acknowledgments

Our investigation depends heavily on the wind-tunnel tests planned and executed by K. Y. Narayana, H. S. Sundaramurthy, and G. Rajendra of National Aerospace Laboratories, Bangalore, India; and P. Srinivasa, B. S. Varambally, A. E. Sivaramakrishnan, S. Pandian, Avinash Kumar, and A. N. Subash of the Aerothermal Test Facility, Vikram Sarabhai Space Center, Trivandrum, India. Multidimensional surface fittings were performed by Avinash Kumar and S. Pandian. Finally, thanks are also due to T. S. Prahlad, the earlier Group Director (Aeronautics), who was instrumental in organizing this multidisciplinary teamwork.

References

[1]Chubb, W., "The Collision Boundary Between the Two Separating Stages of the SA-4 Saturn Vehicles," NASA TN-D-598, Aug. 1961.

[2]Dwork, M., "Coning Effects Caused by Separation of Spin Stabilized Stages," *AIAA Journal*, Vol. 1, No. 11, 1963, pp. 2639, 2640.

[3]Wilke, R. O., "Comments on Coning Effects Caused by Separation of Spin Stabilized Stages," *AIAA Journal*, Vol. 2, No. 7, 1964, p. 1358.

[4]Waterfall, A. P., "A Theoretical Study of the Multispring Stage Separation System of the Black Arrow Satellite Launcher," Royal Aerospace Establishment, TR-68206, Farnborough, Hants, England, UK, Aug. 1968.

[5]Longren, D. R., "Stage Separation Dynamics of Spin Stabilized Rockets," *Journal of Spacecraft and Rockets*, Vol. 7, No. 4, 1970, pp. 434–439.

[6]Subramanyam, J. D. A., "Separation Dynamics Analysis for a Multistage Rocket," *Proceedings of the International Symposium on Space Science and Technology*, edited by S. Kobayashi, AGNE, Tokyo, Japan, 1973, pp. 383–390.

[7]Prahlad, T. S., "A Profile of Aerodynamic Research in VSSC with Application to Satellite Launch Vehicles," *Sadhana*, Vol. 12, Pts. 1, 2, 1988, pp. 125–182.

[8]Sundaramurthy, H., Narayan, K. Y., Suryanarayana, G. K., Lochan, R., Sasidharan Nair, K. G., and Varambally, B. S., "Wind Tunnel Investigation of Strap-On Booster Separation Characteristics of a Launch Vehicle," *Journal of Aeronautical Society of India*, Vol. 38, No. 4, 1986, pp. 215–221.

[9]Lochan, R., Adimurthy, V., and Kumar, K., "Separation Dynamics of Strap-On Boosters," *Journal of Guidance, Control, and Dynamics*, Vol. 15, No. 1, 1992, pp. 137–143.

[10]Moraes, P., Jr., Zdravistch, F., and Azevedo, J. L. F., "Aerodynamics of the Brazilian Satellite Launch Vehicle (VLS) During First Stage Separation," *Proceedings of the AIAA 8th Applied Aerodynamics Conference*, AIAA, Washington, DC, 1990, pp. 904–909 (AIAA Paper 90-3098).

[11]Singh, K. P., Prahlad, T. S., and Deshpande, S. M., "Numerical Simulation of Inviscid Supersonic Flow Over a Launch Vehicle with Strap-On Boosters," AIAA Paper 87-0213, Jan. 1987.

[12]Lumin, Z., Zechu, Y., and Yongjian, Y., "Numerical Simulation of Inviscid Supersonic Flow Over Multiple Bodies," *Proceedings of the AIAA 8th Applied Aerodynamics Conference*, AIAA, Washington, DC, 1990, pp. 910–916 (AIAA Paper 90-3099).

[13]Decker, J. P., "Aerodynamic Abort-Separation Characteristics of a Parallel-Staged Reusable Launch Vehicle from Mach 0.60 to 1.20," NASA TM X-1174, Nov. 1965.

[14]Decker, J. P., and Pierpont, P. K., "Aerodynamic Separation Characteristics of Conceptual Parallel-Staged Reusable Launch Vehicle at Mach 3 to 6," NASA TM X-1051, Jan. 1965.

[15]Orlik-Ruckemann, K. J., LaBerge, J. G., and Hanff, E. S., "Supersonic Dynamic Stability Experiments on the Space Shuttle," *Journal of Spacecraft and Rockets*, Vol. 9, No. 9, 1972, pp. 655–660.

[16]Decker, J. P., and Gera, J., "An Exploratory Study of Parallel-Stage Separation of Reusable Launch Vehicles," NASA TN D-4765, Oct. 1968.

[17]Orlik-Ruckemann, K. J., and Iyengar, S., "Example of Dynamic Interference Effects Between Two Oscillating Vehicles," *Journal of Spacecraft and Rockets*, Vol. 10, No. 9, 1973, pp. 617–619.

[18]Lanfranco, M. J., "Wind-Tunnel Investigation of the Separation Manoeuvre of Equal Sized Bodies," *Journal of Spacecraft and Rockets*, Vol. 7, No. 11, 1970, pp. 1300–1305.

[19]Decker, J. P., and Wilhite, A. W., "Technology and Methodology of Separating Two Similar Size Aerospace Vehicles Within the Atmosphere," AIAA Paper 75-29, Jan. 1975.

[20]Sundaramurthy, H., Suryanarayana, G. K., Lochan, R., Sivaramakrishnan, A. E., and Pandian, S., "Wind Tunnel Simulation of Multi-Booster Separation Trajectories of a Launch Vehicle," *Journal of Spacecraft and Rockets*, Vol. 32, No. 3, 1995, pp. 561–563.

[21]Sundaramurthy, H., Nagarajan, V., and Vasudeva, N. S., "A Wind-Tunnel Test Rig for Multi-Booster Separation Trajectory Studies," National Aeronautical Lab., NAL PD AE 8530, Bangalore, India, Dec. 1985.